Selective Aging of the Human Cerebral Cortex Observed *in Vivo*: Differential Vulnerability of the Prefrontal Gray Matter

Naftali Raz, Faith M. Gunning, Denise Head, James H. Dupuis, John McQuain, Susan D. Briggs, Wendy J. Loken, Allen E. Thornton and James D. Acker[1]

Department of Psychology, The University of Memphis and [1]Baptist Memorial Hospital, Memphis, TN 38152, USA

In a prospective cross-sectional study, we used computerized volumetry of magnetic resonance images to examine the patterns of brain aging in 148 healthy volunteers. The most substantial age-related decline was found in the volume of the prefrontal gray matter. Smaller age-related differences were observed in the volume of the fusiform, inferior temporal and superior parietal cortices. The effects of age on the hippocampal formation, the postcentral gyrus, prefrontal white matter and superior parietal white matter were even weaker. No significant age-related differences were observed in the parahippocampal and anterior cingulate gyri, inferior parietal lobule, pericalcarine gray matter, the precentral gray and white matter, postcentral white matter and inferior parietal white matter. The volume of the total brain volume and the hippocampal formation was larger in men than in women even after adjustment for height. Inferior temporal cortex showed steeper aging trend in men. Small but consistent rightward asymmetry was found in the whole cerebral hemispheres, superior parietal, fusiform and orbito-frontal cortices, postcentral and prefrontal white matter. The left side was larger than the right in the dorsolateral prefrontal, parahippocampal, inferior parietal and pericalcarine cortices, and in the parietal white matter. However, there were no significant differences in age trends between the hemispheres.

Introduction

A claim that the human brain is altered by aging is unlikely to provoke a debate, and few would argue that the effects of age on brain structure are uniform and diffuse. What remains unsettled are more complex questions regarding specific patterns of cerebral aging and their underlying mechanisms. It is unclear whether coherent common patterns of localized brain changes emerge in the normal aging population, or whether each individual brain develops into a unique patchwork of regions characterized by variable degree of stability and decline. It is also unclear at which levels of neural and functional organization this selective vulnerability is expressed: individual cells and their organelles, cortical lamina, specific nuclei, cytoarchitectonically distinct cortical regions, neurotransmitter systems, vascular networks, or all of the above and more. Finally, if clear regional differences do emerge in the aging brain, the question then is what are the mechanisms that produce them, and what are the functional sequelae of differential brain aging? In this report, we examine the topography of age-related structural differences in the human cerebral cortex using *in vivo* evidence from magnetic resonance imaging (MRI), and offer some speculations on the origins of these differences.

Post-mortem (PM) studies of mammalian brains suggest that aging of specific regions and nuclei is heterochronic (see Flood and Coleman, 1988 for review). Specifically, in the mammalian cerebral cortex, there may be a gradient of aging from the association areas to the primary sensory regions. In the past two decades, noninvasive neuroimaging has been developed to complement PM findings by providing description of the brain structure and function *in vivo*. Such description lacks the histological precision of PM studies, and at first, structural neuroimaging yielded only nonspecific neuroanatomical markers of senescence – cerebral ventriculomegaly and generalized shrinkage of the cerebral parenchyma (Freedman, 1984; Jernigan *et al.*, 1990). Nevertheless, in addition to these nonspecific findings, a cumulative record of structural MRI studies reveals clear regional heterogeneity: some brain structures show substantial age-related declines, while other locales are relatively spared. First of all, a distinction between aging of gray and white matter is apparent. The preponderance of MRI data indicate that although microstructural changes in the white matter are significant (Raz *et al.*, 1990; Wahlund *et al.*, 1990), there is no significant age-related loss of the total white matter volume (e.g. Jernigan *et al.*, 1990; Pfefferbaum *et al.*, 1992, 1994; Raz *et al.*, 1993a; Blatter *et al.*, 1995). In contrast, age differences in the total gray matter volume are substantial (Jernigan *et al.*, 1990; Pfefferbaum *et al.*, 1992, 1994).

To date, regional differences in brain aging have not been investigated in a systematic manner across a large number of regions and specimens. The evidence from numerous PM and *in vivo* studies suggests, however, that the prefrontal (e.g. Brody, 1955; Haug, 1985; Coffey *et al.*, 1992; Raz *et al.*, 1993a; Cowell *et al.*, 1994; DeCarli *et al.*, 1994), the entorhinal (Arriagada *et al.*, 1992; Heinsen *et al.*, 1994), and the temporal (Terry *et al.*, 1987; Cowell *et al.*, 1994; Sullivan *et al.*, 1995) cortices are the most severely affected, whereas the primary visual and primary somatosensory cortices may be more resistant to the influence of age (see Kemper, 1994, for a review of human postmortem literature, and Raz, 1996, for a review of the MRI findings). Age-related changes in the hippocampal formation were observed in many animal studies (reviewed by Flood and Coleman, 1988), human PM studies (reviewed by Kemper, 1994) and MRI investigations (reviewed by Raz, 1996). Nevertheless, in some samples no significant age effects on hippocampal pyramidal neurons were found (Flood *et al.*, 1987; West, 1993), and a recent neuroimaging report suggested a total lack of age-related changes in hippocampal formation in a sample of healthy men (Sullivan *et al.*, 1995).

Functional imaging studies of the aging brain corroborate, at least in part, the structural MRI findings. Whereas studies of age-related differences in regional cerebral blood flow (rCBF) reveal no age differences in the total brain blood flow, they yielded data that show differential age-related decline in blood flow to the prefrontal cortex and little change in the occipital and temporal cortices (see Waldemar, 1995, for a review).

Two factors may modify the regional distribution of age-related changes in the cerebral cortex: sex and hemispheric asymmetry. The brain is a sexually dimorphic organ (Goy and McEwen, 1980), and aging may be a sexually dimorphic process as well. In general, males are more vulnerable than females to a

wide spectrum of central nervous system insults (Gualtieri and Hicks, 1985). Such selective vulnerability is observed at the early perinatal period, and may be attributed to differential maturation of the sexes (Raz *et al.*, 1994, 1995). It is plausible that males are also more likely to experience adverse age-related changes. Although gender-specific patterns of brain aging were reported in few studies, men usually fare worse than women. They show greater age-related declines in the volume of the temporal lobe (Cowell *et al.*, 1994), the dorsolateral prefrontal cortex (Raz *et al.*, 1993a) and the hippocampal formation (de Toledo-Morrell *et al.*, 1995), as well as greater age-dependent increase in relative volume of cerebrospinal fluid (CSF) (Condon *et al.*, 1988) and in lateral ventricular size (Gur *et al.*, 1991), and greater thinning of the corpus callosum (Unsal *et al.*, 1995). There are two notable exceptions to this trend. In a recent study of normal volunteers (Blatter *et al.*, 1995), men evidenced very modest declines in both gray and white matter volume ($r = -0.26$ and $r = -0.24$ respectively), whereas for women a clear discrepancy in age trends was observed: $r = -0.39$ for gray and $r = 0.05$ for white. In another study (Breteler *et al.*, 1994) women showed significantly higher prevalence of MRI white-matter hyperintensities (WMH) than men.

The mammalian brain is an asymmetrical structure (see LeMay, 1985, and Galaburda, 1995, for reviews), and the development of its hemispheres may be asynchronous (Best, 1988). One of the strongest and most consistent indices of hemispheric asymmetry across the extant mammalian species and the fossil records are frontal and occipital petalia – protrusion of the right frontal and left occipital poles – that give many brains an appearance of being torqued around the central axis (LeMay, 1977, 1985). A number of researchers proposed that inherently asymmetric brains may evidence hemisphere-specific pattern of aging as well. With virtually no neuroanatomical data to bear on the subject, physiological and behavioral evidence pertinent to the hemi-aging hypothesis is equivocal (see review by Lapidot, 1983). Most of the electrophysiological findings summarized by Lapidot point to a more rapid deterioration of the left hemisphere, whereas the results of cognitive studies are interpreted as evidence of right hemi-aging. However, a more recent series of information processing experiments indicates that when the task difficulty is equated, no specific age-related lateralized deficit pattern can be discerned (Nebes, 1990).

Although the hypothesis of differential aging of the cerebral cortex is intriguing, it rests on findings from studies that were limited in the scope of surveyed cortical regions, and in the number of examined subjects or specimens. In a few prospective *in vivo* investigations of cortical regions in healthy normal adults (Jernigan *et al.*, 1991; Pfefferbaum *et al.*, 1994; Cowell *et al.*, 1994), the investigators sampled, outlined and measured cortical regions using computerized automatic methods. Although this approach saves time and ensures objectivity, it results in arbitrary division of the cerebral volume, sometimes based on very limited neuroanatomical rationale. Cortical regions which may differ in susceptibility to aging are lumped together, and potential evidence of differential cortical shrinkage is thereby obscured. In addition, in most of the *in vivo* studies of normal brain structure, the regions of interest included both white and gray matter, ignoring the possibility of differential aging of these two cerebral components. A more recent study in which some of these problems were alleviated (Sullivan *et al.*, 1995) dealt only with the temporal lobe structures.

The studies of brain aging *in vivo* evidenced a number of

additional methodological limitations. With some rare exceptions, they were conducted on relatively small samples. In some of these samples, young persons (under the age of 40) were clearly overrepresented (Cowell *et al.*, 1994), others (Sullivan *et al.*, 1995) were restricted to men. In some instances, the sparseness of the MRI data obtained from relatively thick slices threatened the validity of regional measures (Raz *et al.*, 1993a; Cowell *et al.*, 1994). In virtually all MRI studies of the aging brain to date, the asymmetry measures could have been influenced by uncorrected changes in subject's head position (Zipursky *et al.*, 1990). Finally, because the test of the hemi-aging hypothesis and assessment of differential sex effects depend on the significance of the hemisphere (or sex) × age interaction, maintaining adequate statistical power calls for larger samples than are usually available for neuroimaging studies (Cohen, 1988).

In this study, we address the following major questions. First, are the association cortices more vulnerable than primary sensory cortices to the effects of aging? Second, do men suffer disproportionally greater age-related cortical changes than women? Third, is there a clear lateralized pattern of cortical aging? Our objective was to address the question of differential aging of the cerebral cortex directly, within a unified framework of a prospective *in vivo* investigation in a relatively large sample with a balanced gender composition. To ensure attribution of the findings to normal aging rather than to age-related pathology, we screened out individuals with known health problems, and even those with a moderate level of emotional distress. We used highly reliable volumetric measures that have been developed and tested in our previous studies (Raz *et al.*, 1993a,b, 1995) to estimate the volume of specific brain regions that were demarcated manually, based on clearly specified rules and easily identifiable neuroanatomical markers. To ensure unbiased measures of hemispheric asymmetry we acquired images with a volume MRI sequence which permitted off-line adjustment for head rotation, tilt and pitch.

Materials and Method

Subjects

The data for this study were collected in an ongoing investigation of neuroanatomical correlates of age-related differences in cognition. Subjects were recruited by advertising in local media and on the University of Memphis campus. They were screened using an extensive health questionnaire for history of cardiovascular, neurological and psychiatric conditions, head trauma, thyroid problems and diabetes. Subjects who reported a history of treatment for drug and alcohol problems or admitted to taking more than three alcoholic drinks per day were excluded from the study. Twelve subjects (five men and seven women, aged 48–77 years) who reported a history of mild hypertension were admitted as their blood pressure was successfully controlled by medication. As suggested in the literature, people who adhere to a medication regiment and control their hypertension are no more likely to exhibit signs of cerebrovascular disease than normotensive elderly (Fukuda and Kitani, 1995). In addition, the sample was screened for cerebrovascular disease by inspection of white matter hyperintensities on the MRI scans (see below for details). This procedure virtually eliminated hypertension as a risk factor, for only in persons with very substantial white matter hyperintensities is blood pressure predictive of the volume of leukoaraiotic lesions (DeCarli *et al.*, 1995). Of 166 subjects who underwent MRI, all or substantial portions of the data for six subjects were lost due to technical problems such as disk failure, excessive movement artifacts, operator error and (in two cases) significant discomfort to the subject during scanning.

All subjects were screened for dementia and depression using a modified Blessed Information-Memory-Concentration Test (BIMCT, Blessed *et al.*, 1968) and Geriatric Depression Questionnaire (CES-D, Radloff, 1977). For BIMCT we used a cut-off score of 30 correct out of

possible 34, whereas for CES-D the cut-off score was 15. The average BIMCT score was 32 ± 1 correct, and there was no correlation between the score and age: $r = 0.01$. The average CES-D score in the sample was 5.13 ± 5.09, indicating a very low level of overt emotional distress in this sample, and the correlation between CES-D score and age was $r = -0.12$ (NS). The average education was 15.77 years for the men and 15.86 for the women. The correlation between education and age was $r = 0.09$ (NS). All subjects were strongly right-handed as measured by the Edinburgh Handedness Questionnaire (Oldfield, 1971). Finally, all subjects admitted to the study had their MRI scans examined by an experienced neuroradiologist (J.D.A.) for signs of space-occupying lesions and cerebrovascular disease. After this examination 10 subjects (six men and four women, all >65 years of age) were removed from the sample because of signs of mild to moderate cerebrovascular disease (numerous punctate lesions, lacunar infarcts, significant unilateral concentration of white-matter hyperintensities).

The final sample consisted of 148 healthy adults with age range 18–77 years, and mean age 46.47 ± 17.17 years. There were 82 women (age 45.72 ± 16.48 years), and 66 men (age 47.39 ± 18.07 years). The age distribution was approximately rectangular, and did not differ between the sexes, nor was the mean age difference significant ($t < 1$).

MRI Protocol
Imaging was performed at the Diagnostic Imaging Center, Baptist Memorial Hospital, Memphis, TN on a 1.5 T Signa scanner (General Electric Co., Milwaukee, WI). Initially, three contiguous sagittal images of the brain were obtained $T_E = 16$ ms, $T_R = 400$ ms, slice thickness = 5.0 mm. After examination of the scout images, the subject's position was verified and adjusted, and a volume image was acquired using T_1-weighted three-dimensional spoiled gradient recalled acquisition sequence (SPGR). For each subject, 124 contiguous axial slices were acquired with $T_E = 5$ ms, and $T_R = 24$ ms, FOV = 22 cm, acquisition matrix 256 × 192, slice thickness = 1.3 mm, and flip angle = 30°. After the SPGR sequence a fast spin echo (FSE) sequence of interleaved T_2 and proton-density weighted axial images was acquired to be used in screening for age-related cerebrovascular disease. In this sequence the parameters were: $T_R = 3300$ ms, effective $T_E = 90$ ms, for T_2 slices and effective $T_E = 18$ ms, for proton density slices. Slice thickness was 5 mm, and interslice gap was 1.5 mm.

Reformatting and Alignment of MR Images
After acquisition, the SPGR images were transferred to the General Electric Independent Console for off-line reformatting. One of the objectives of reformatting was to correct the image for undesirable effects of head tilt, pitch and rotation. Images were reformatted with General Electric proprietary software (version 3.0). Standard neuro-anatomical landmarks were used to bring each brain into a unified system of coordinates, and to correct the deviations in all three orthogonal planes. In this standard position, the sagittal plane cut through the middle of the interhemispheric fissure. The axial plane passed through the anterior–posterior commissure (incorporating the AC–PC line) and through the orbits, perpendicular to the sagittal plane. The coronal plane was leveled by the orbits and the auditory canals, and passed perpendicular to the axial. Reformatted images were cut into sections 1.5 mm apart and saved on a VHS tape. The thickness of the reformatted slices was 0.86 mm (one linear pixel).

Computerized Analysis of the MRI Scans
Morphometry was performed using JAVA software (Jandel Scientific Co., San Rafael, CA). The MRI images were transferred to the VHS tape and digitized via a TARGA M-8 frame-grabber board (AT&T Corp., Murray Hill, NJ). A trained operator displayed each image on the video monitor screen with standard brightness and contrast, and outlined the areas of interest (AOI) using a digitizing tablet. The areas were computed by JAVA software, and the volumes of regions of interest (ROIs) were calculated using the basic volume estimate (Uylings et al., 1986), which amounts to a sum of the AOI areas multiplied by the inter-slice distance. All measures were calibrated using a standard ruler bar provided on the MRI scans along the image, and volumes were computed in cubic centimeters (cm³).

Delineation of the ROIs
Trained operators who were blind to the subjects' exact age and sex

manually traced all ROIs. The set of slices containing each ROI was split into two equal groups at random, and each half-sample was traced by a different operator. In occasional regions of partial voluming, the operator interpolated the line between two clearly definable segments of the cortical border. We resolved all questionable cases by consulting the correlative and general brain atlases (DeArmond et al.,1976; Duvernoy, 1988; Montemurro and Bruni, 1988; Nieuwenhuys et al., 1988; Ono et al., 1990; Talairach and Tournoux, 1988). Our approach is similar although not identical to the cortical parcellation methodology developed by Rademacher et al. (1992). The identification and tracing rules were anchored in neuroanatomical markers, and geared towards reliable, conservative sampling of the ROIs, which therefore included less than the totality of the structure they denoted, but avoided encroachment into other ROIs. Our approach to definition of the ROIs is more faithful to anatomic distinctions than fully automated approaches that divide the brain into arbitrary geometrically defined segments, although it still falls short of strictly neuroanatomical parcellation. The latter, designed along the lines proposed by Rademacher and colleagues, would require more painstaking attention to specific sulcal patterns on a three-dimensional surface rendering. Such three-dimensional assistance was unavailable in our software. The following ROIs were identified, traced and measured according to the rules outlined below, a compendium of which is available upon request. In brief, the rules of ROI demarcation relied on a set of neuroanatomical markers which ideally should have been sufficient for ROI definition. However, constraints on white–gray matter separation (e.g. high density of convolutions in the proximity of the frontal pole) and lack of obvious landmarks forced us to modify this approach by cutting the structure according to fixed percent-of-volume criteria in cases when reliable determination of the boundaries was impossible. The importance of not encroaching onto other structures and preserving the highest possible reliability took precedence over the desire to obtain the most complete and accurate description of a given anatomical region.

Reformatting produced between 93 and 114 coronal slices per subject, and tracing all of them would have been prohibitively time-consuming. Therefore, we estimated the volume of each cerebral hemisphere from coronal slices separated by 4.5 mm gaps (every third slice sampled). In addition, the areas of the three most rostral and three most caudal slices sampled with a 1.5 mm gap were measured to evaluate frontal and occipital petalia. Thus, the total volume of the hemispheres was determined on the basis of 37–44 sections. Gray and white matter were included in traced hemispheres, whereas cerebral ventricles, midbrain, cerebellum and pons were excluded. To analyze the pattern of the frontal and occipital petalia, we examined three most anterior and three most posterior slices of the whole brain, and computed the asymmetry index by subtracting the left volume from the right and normalizing by their average volume.

The volume of the dorsolateral prefrontal cortex (DLPFC) was computed from 10–13 coronal slices separated by 1.5 mm gaps and located rostrally to the genu of corpus callosum. This ROI included superior, middle and inferior frontal gyri and covered Brodmann areas 8, 9, 10, 45, 46. The DLPFC was defined as the gray matter located between the most dorsomedial point of the cortex and the orbital sulcus. We estimated the volume of the orbitofrontal cortex (OFC) from the same slices, using the most lateral branch of the orbital sulcus as the lateral boundary and the olfactory sulcus as the medial boundary. The OFC included parts of Brodmann areas 11 and 47. Thus, OFC and DLPFC were complementary parts of an ROI labeled the prefrontal cortex (PFC).

To determine the range of inclusion, we calculated the number of slices from the frontal poles to the slice immediately rostral to the genu of the corpus callosum. The operators measured the DLPFC and the OFC on the caudal 40% of these slices. Only the continuous cortical ribbon was measured; gray matter was excluded if it was completely enclosed by white matter. Examples of coronal slices used to estimate the DLPFC and the OFC volume are shown in Figure 1A.

Anterior cingulate gyrus (ACG) was measured on four coronal slices in the same series of slices that was used for DLPFC measures. This shorter series incorporated 16% of the total number of slices rostral to the genu of the corpus callosum. The anterior cingulate gyrus was defined as all gray matter falling between the inferior and superior cingulate sulci, and corresponded approximately to the most anterior part of the
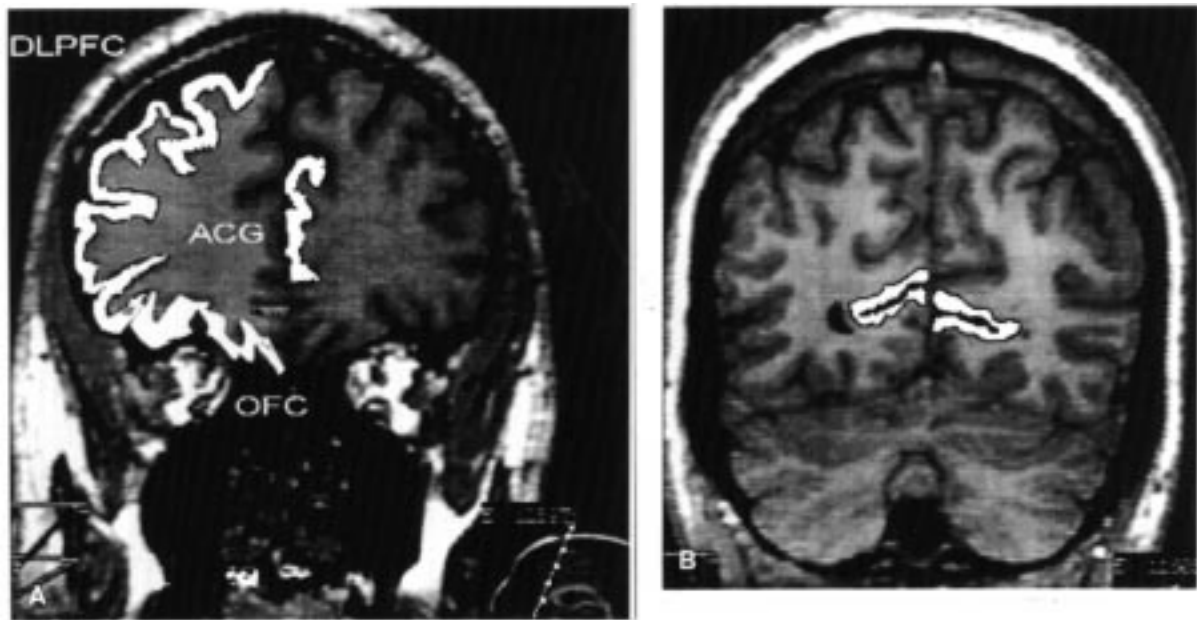
Figure 1. Regions of interest highlighted on coronal slice: (A) dorsolateral prefrontal (DLPFC); orbito-frontal (OFC) and anterior cingulate cortex (ACG); (B) primary visual cortex (VC).
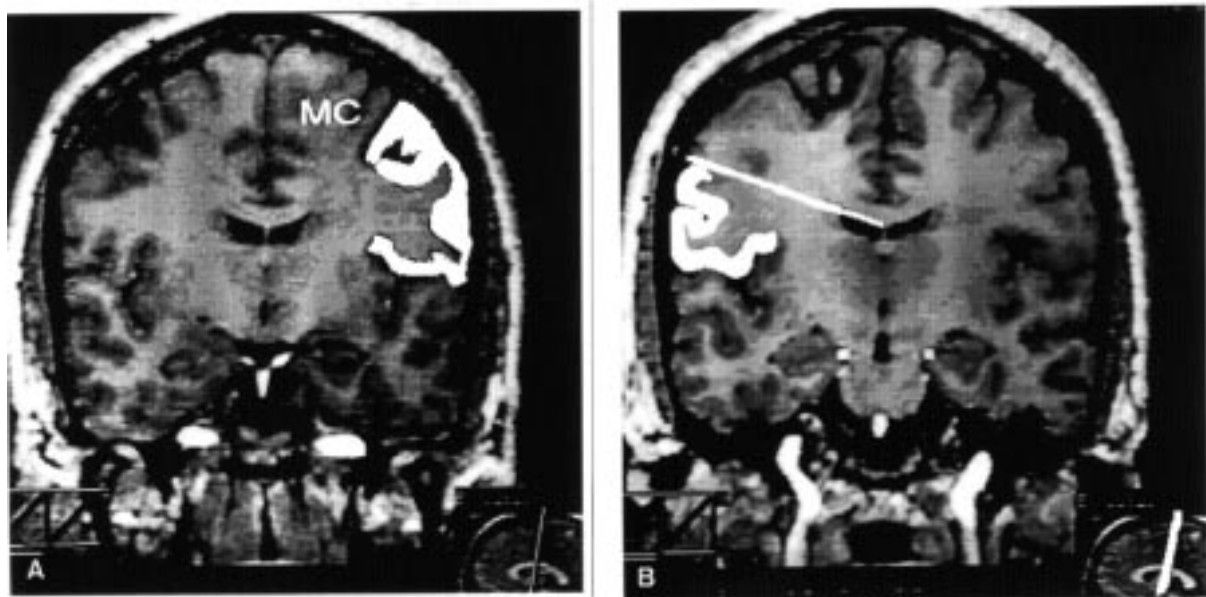

Figure 2. Coronal slices with ROIs highlighted: (A) precentral gyrus (primary motor cortex); (B) primary somatosensory cortex (SSC), with the line indicating implementation of the 'ventricle rule'.

Brodmann area 24 or prelimbic area. Examples of anterior cingulate gyrus tracing are shown in Figure 1A.

Prefrontal white matter volume was estimated from five to seven coronal slices separated by 3 mm gaps. The total hemispheric white matter area was measured on every other slice from the sequence described above. The frontal horns of the lateral ventricles as well as any gray matter enclosed within the white matter were excluded from the prefrontal white matter measure.

The volume of the precentral gyrus (including primary motor cortex, MC) was estimated from four to six coronal sections separated by 1.5 mm gaps. The range of slices was defined as the rostral 75% of the number of slices between the anterior commissure to the mammillary bodies. To

locate the superior boundary of the precentral gyrus, a line was drawn along the dorsal surface of the lateral ventricle and extended to the surface of the cortex (Figure 2B). The precentral sulcus was identified as the first major sulcus located at or below the intersection of the line with the cortical ribbon, while the most superior branch of the lateral sulcus served as the inferior boundary. Therefore, the whole precentral gyrus was not included in the ROI, nor did all of the ROI volume represent the primary motor cortex. Thus, precision of area representation was sacrificed for improved reliability. Nevertheless, the ROI represented most of the precentral gyrus, and covered a substantial part of the primary motor cortex (Brodmann area 4). Examples of precentral gyrus tracings are presented in Figure 2A.
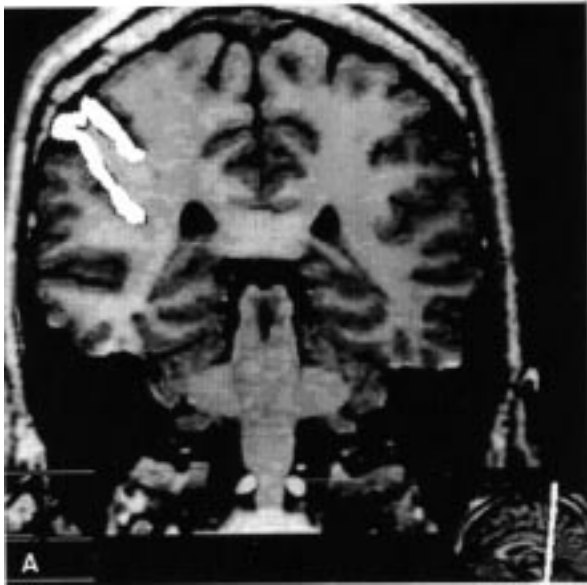
Figure 3. Coronal slices with (A) inferior parietal lobule (IPL), and (B) superior parietal cortex (SPC) highlighted.
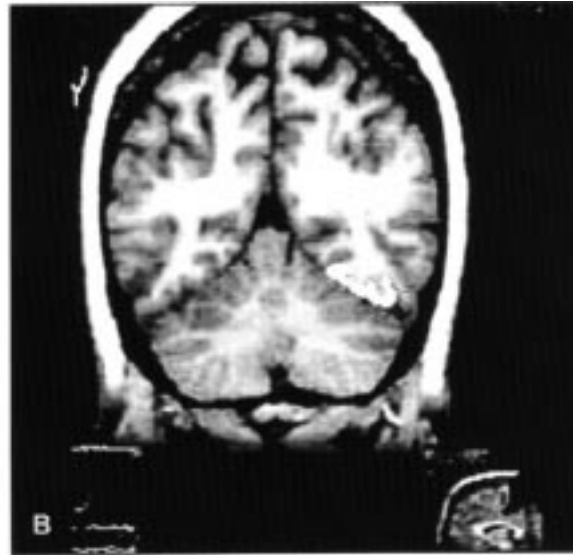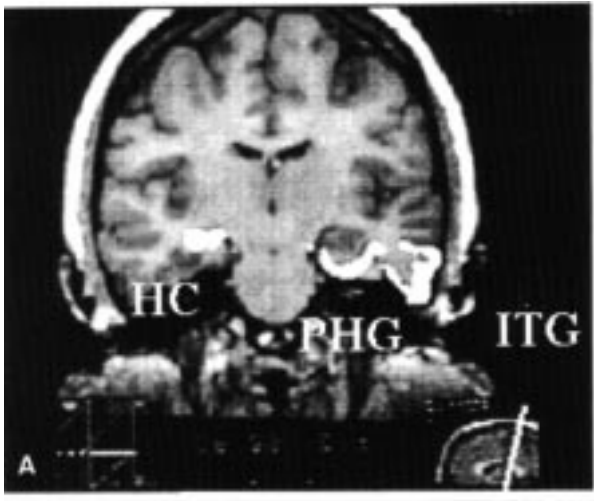

Figure 4. Coronal slices with the temporal-occipital ROIs highlighted: (A) inferior temporal (ITG) and parahippocampal (PHG) gyri, and the hippocampal formation (HC); (B) fusiform gyrus (FG).

The borders of the postcentral gyrus (including primary somatosensory cortex, SSC) are the central sulcus, the Sylvian fissure and the postcentral sulcus. The volume of the postcentral gyrus was estimated from six to nine coronal slices sampled with 1.5 mm gap. The range of slices was determined by taking the rostral 50% of the slices between mammillary bodies and the posterior commissure. To establish the superior and inferior limits, the same rules as for the precentral gyrus were applied. The selection, demarcation and measurement approach to this ROI were similar to those used for the precentral gyrus. This ROI corresponded approximately to Brodmann areas 1–3, and is depicted in Figure 2B.

The volume of the inferior parietal lobule (IPL) was estimated from five to ten coronal slices, 1.5 mm apart. We determined the range of slices by taking the rostral 65% of the slices between the posterior commissure to the slice immediately caudal to the end of the splenium of the corpus callosum. To locate the superior boundary of the IPL, an operator drew a

line along the dorsal surface of the lateral ventricle, extending it to the surface of the cortex. The IPL was demarcated by the first major sulcus located at or slightly above the intersection of the line with the cortical ribbon – the postcentral sulcus. The most superior branch of the lateral sulcus served as the inferior boundary. The borders of this ROI included mainly Brodmann area 40 (see Figure 3A for an example).

The volume of the superior parietal cortex (SPC) was estimated from the slices ranging across the rostral 65% of the distance between the posterior commissure and the splenium of the corpus callosum (as in IPL volume estimate). The superior cingulate sulcus, which is located on the medial border of the central sulcus, was used as the superior boundary of this ROI. All cortex between this and the inferior boundary is included. To determine the inferior boundary, the ventricle rule (see IPL, SSC and MC demarcation rules above) was applied to demarcate the largest sulcus or major branch of a sulcus) at or slightly above where the ventricle line crosses the lateral cortex. In practice, this included all cortex superior to

that demarcated as the IPL, mainly Brodmann area 7, as depicted in Figure 3*B*.

The volume of pericalcarine (visual) cortex (VC) was estimated as the volume of the cortical ribbon lining the calcarine sulcus. This sulcus appeared as the most ventromedial sulcus in the temporo-occipital cortex at the coronal slice that is mid-vermis or immediately caudal to mid-vermis. The range of the VC extended through the caudal coronal slices, but because the high density of convolutions on the caudal slices precluded reliable measurement, VC was measured on the anterior 50% of the coronal slices between the mid-vermis slice and the occipital pole (13–15 coronal slices, 1.5 mm apart). The inferior and superior boundaries of this ROI were defined as the point at which the opening of the sulcus occurred. At this point a line was drawn horizontally so that no cortex (dorsal or ventral) outside of the calcarine sulcus was included. This ROI contained mainly the primary visual cortex (Brodmann area 17) and probably some secondary visual areas (Brodmann area 18) as well. An example of VC tracings is presented in Figure 1*B*.

The volume of several parietal white matter ROIs (precentral, postcentral, inferior and superior parietal) was estimated from 18–25 coronal slices separated by 1.5 mm gaps. These were the same slices that were used for measurement of the MC, SSC, IPL and SPC.

Parahippocampal gyrus (PHG) volume was estimated from 25–30 coronal slices, 1.5 mm apart. The first slice was the one on which the temporal stem became discernable; while the most caudal slice that showed the pulvinar was the last in the series. The superior border was a horizontal line drawn from the most medial point of the PHG white matter to the cortex, whereas the inferior border was the most inferior line drawn from the most inferior point of the collateral sulcus to the white matter. To discriminate the HC and PHG, the subiculum was excluded from the PHG. Reliable demarcation between the perirhinal and entorhinal cortex was not feasible due to substantial complexity and individual variability in these structures (Insausti *et al.*, 1995). This ROI included almost the entire entorhinal cortex (Brodmann area 28) as well as additional PHG area (see Figure 4*A* for an example of PHG tracing).

Inferior temporal gyrus (IT) volume was estimated from 20–28 coronal slices separated by 1.5 mm, and ranging from the mammillary bodies to the last slice containing the splenium of the corpus callosum. This ROI encompassed all the gray matter between the inferior temporal and occipitotemporal sulci, corresponding to the Brodmann area 20, as depicted in Figure 4*A*.

The fusiform gyrus (FG), which spans temporal and occipital lobes, was measured in two steps. First, the areas of the ROI were obtained from successive coronal slices beginning with the level of the anterior commissure to the last slice on which the splenium of the corpus callosum was present. After that, the posterior fusiform gyrus range was determined by counting the number of slices between the occipital poles and the most anterior slice on which the splenium is no longer present, and taking 33% of that range. On the slices anterior to the most caudal point of the splenium, the lateral boundary of the FG was the occipitotemporal sulcus. Starting at the first slice retrosplenial slice, the lateral boundary was the most ventro-lateral sulcus. In most (but not all) cases this was the occipitotemporal sulcus. The medial boundary of the FG was the collateral sulcus. In the posterior portion of the FG the collateral sulcus bifurcates into the most medial (lingual) sulcus and was not traced. At that point, the collateral sulcus becomes the most lateral sulcus, and it is used as the medial boundary. The sulci were 'cut' by bisecting the boundary sulcus so as to create the internal aspects of the sulcus even if they were not present. The FG as demarcated here covered Brodmann areas 37 and 19 (inferior part). An example of FG tracing is presented in Figure 4*B*.

Hippocampal formation (HC) was measured on a series of 19–25 coronal slices. As we were unable to separate the hippocampus proper from the rest of the formation, we use the term hippocampus only as a matter of convenience. The mammillary bodies defined the rostral boundary of the HC; its caudal boundary was marked by the slice showing the fornices rising from the fimbria. Care was taken not to include the amygdala in this ROI. The examples of tracing of the HC are presented in Figure 4*A*.

We assessed reliability of the volume measures using intraclass correlation [ICC(3), Shrout and Fleiss, 1979]. The ICC(3) is applicable to a fixed set of raters, and it takes into account both the inter-rater

agreement on the linear order of the measured objects (as does the Pearson correlation coefficient), and the absolute size of each measured object (as does the *t*-test). The ICC(3) for each ROI was based on tracings by two operators who were selected from a group of eight. To achieve high reliability, the operators were trained, side-by-side, on a random set of brains until they reached good agreement on interpretation of the rules. After agreement was reached, each operator traced another randomly selected set of 6–12 brains independently from the total sample of 43 brains available from our database at that time. Only pairs of operators who achieved desirable level of reliability (ICC ≥ 0.90) traced given ROIs. The reliability coefficients ranged from 0.90 for the precentral gyrus volume to 0.99 for the volume of the prefrontal white matter, the cerebral hemispheres and the hippocampus. The median reliability coefficient was ICC(3) = 0.94.

Results

The hypotheses concerning age trends, sex differences and hemispheric asymmetry were tested within a general linear model framework. The volumes of each ROI and the whole brain served as dependent variables in 17 linear models, with sex as a grouping factor, age as a continuous independent variable, and height as a covariate. Hemisphere (right versus left) was treated as a repeated measure.

Height was introduced into the models to control for the influence of body size on the volume of the brain and its regions. Although there was no association between age and body size within the sexes ($r = 0.00$ for men, and $r = 0.05$ for women), men, as expected, were taller than women: 178.19 versus 165.35 cm, $t(146) = 11.98$, $P < 0.001$. Men also had larger heads [$t(146) = 5.18$, $P < 0.001$], and covarying head size could have been an alternative way of controlling for sexual dimorphism in body size. We opted for height as a covariate for the following reason.

In early development, brain growth contributes directly to the increase in head size, and in adults, head size is closely related to the volume of the brain. In our sample, the two variables correlated ($r = 0.47$ for men and $r = 0.56$ for women), even though one (head) was represented by a cross-sectional area on a single midsagittal slice and the other (brain) by the volume computed from coronal slices. Removal of the variance associated with the head size from the ROI volume would have eliminated a substantial share of the true brain variance. In assessing relations between the size of brain regions and other variables, this variance must be retained. Doing otherwise would amount to over-correction and under-estimation of the true age and sex differences. Head size would be an appropriate covariate in a study of gyral atrophy, in which the goal is to determine changes in cortical mantle relatively to the cranial cavity. The premise of adjusting ROI volumes for head size is that the nonparenchymal part of the brain is CSF accumulated through an atrophic process. Historically, that was the reason for adjustment by computing ROI-to-cranium ratios. In this study, however, the assessment of gyral or ventricular atrophy was not our goal.

The continuous independent variables (age and height) were recentered at their respective means. The interactions between each continuous variable and the grouping factor were tested to check for homogeneity of regression slopes across the groups. If these interactions were nonsignificant, they were removed from the model and the reduced model was fitted to the data. This was the case in all but two models. For the whole brain, primary somatosensory cortex and the hippocampus the homogeneity of slopes assumption was not met (the sex × height interaction was significant at $P < 0.10$ level), and separate linear models were fitted for each sex.

The results of the linear model analyses presented in Table 1

Table 1

Effects of age, sex and hemisphere on cortical ROIs after adjustment for height

Structure	F ratio			Pearson r with age
	Age	Sex	Asymmetry	
Whole brain[a]	44.09***	16.98***	64.97***R	−0.42
Men	28.51***		34.22***R	−0.55
Women	17.54***		30.68***R	−0.41
Prefrontal gray matter	68.17***	1.14	8.46***L	−0.55
Dorsolateral prefrontal cortex	56.13***	0.40	22.58***L	−0.51
Orbito-frontal cortex	45.49***	4.55	13.12***R	−0.48
Anterior cingulate cortex	6.51	2.94	0.04	−0.18
Parahippocampal cortex	6.03	0.75	27.75***L	−0.18
Inferior temporal cortex[b]	25.71***	0.23	1.10(R)	−0.35
Men	19.62***		8.32*(R)	−0.49
Women	6.94*		0.16(R)	−0.24
Fusiform gyrus	25.84***	5.83	13.55***R	−0.35
Hippocampal formation[a]	16.39***	10.83***	2.74(L)	−0.28
Men	5.99		1.74(L)	−0.29
Women	10.78***		0.83(L)	−0.34
Precentral (primary motor) cortex	1.30	3.74	1.25(L)	0.09
Postcentral (primary somatosensory) cortex[a]	14.24***	6.42	2.70(R)	−0.26
Men	7.94*		0.45(R)	−0.33
Women	6.30		3.71(R)	−0.25
Superior parietal cortex	21.52***	0.00	23.97***R	−0.36
Inferior parietal cortex	5.12	0.93	54.19***L	−0.18
Pericalcarine (primary visual) cortex	6.46	6.85*	13.26***L	−0.19
White matter				
Prefrontal	8.97**	5.87	27.01***R	−0.22
Precentral	0.95	2.02	5.40(L)	−0.08
Postcentral	2.51	3.84	13.07***R	−0.12
Superior parietal	6.92**	0.00	7.06*L	−0.22
Inferior parietal	0.00	1.01	73.36***L	−0.00

[a]Sex × height interaction was significant and could not be removed from the model. Separate models were fitted for each sex.

[b]Sex × age interaction was significant and could not be removed from the model. Separate models were fitted for each sex.

*$P < 0.01$; **$P < 0.003$; ***$P < 0.001$. Bonferroni critical $\alpha = 0.003$. Correlations significance: for $|r| > 0.20$, P fs20 0.01; for $|r| > 0.25$, P fs20 0.003; for $|r| > 0.27$, $P < 0.001$.

are summarized below. All significance levels were adjusted for the number of comparisons (17) using Bonferroni correction, and statistical significance was declared for $P < 0.003$. We highlight, however, effects that were significant at the uncorrected 0.01 level limits as well.

Age differences

Although many regions of the cerebral cortex evidenced statistically significant negative age trends, the magnitude of the declines varied widely across the locales. Linear trends for age-related differences in cortical ROIs are depicted (along with the distribution of the measures across the age span) in Figure 5A–C. Except for the orbito-frontal cortex [$F(1,145) = 5.90$, $P < 0.025$] there were no significant deviations from linearity. Although statistically significant, that trend was rather weak, and added only 3.1% of the explained variance.

The steepest age-related trend was observed for the prefrontal gray matter: the dorsolateral and the orbital frontal cortices. Because these ROIs were correlated ($r = 0.60$, $P < 0.001$), we combined them into one ROI: the PFC. This linear trend corresponds to the loss of prefrontal gray matter at an average rate of 4.9% per decade. The similar trend for the superior parietal cortex showed an 4.3% per decade decline, compared to 2% per decade for the hippocampus. We compared Pearson correlations between age and the ROI volumes (Table 1) using Steiger's Z^* statistic, which takes into account the correlation between the variables correlated with age (Steiger, 1980). The correlation between PFC volume and age ($r = -0.55$) was

significantly larger than the next largest correlation, between age and the SPC volume ($r = -0.36$), $Z^* = 2.47$, $P < 0.015$.

Sex differences

Considerable discrepancy in body size could account for sex differences in cortical ROI volume, and this factor had to be taken into account. After body size (stature) was controlled statistically, most ROI volumes did not differ significantly between men and women. There were two notable exceptions: men had significantly larger cerebral hemispheres, and hippocampi even after adjustment for height. There were no significant sex differences in the slopes of age trends ($P > 0.10$ for sex × age interactions) except for the inferior temporal cortex. Age-related differences in the IT volume declines were marginally significant [$F(1,142) = 4.01$, $P < 0.05$ for the interaction effect], with men ($r = -0.49$) being more affected than women ($r = -0.24$).

Cerebral Asymmetry

We observed a small (~1%) but consistent rightward[1] asymmetry of the cerebral hemispheres. (We use the terms 'leftward' and 'rightward' in reference to asymmetry to indicate that the left or the right hemisphere of the ROI is larger.) The hemispheric differences were most prominent in the white matter: rightward for the prefrontal and postcentral gyri, and leftward for the inferior parietal lobule. Prefrontal and parietal gray matter showed a mixed pattern of lateral differences: DLPFC was larger on the left, whereas the OF cortex volume was greater in the right hemisphere, the inferior parietal lobule was decisively
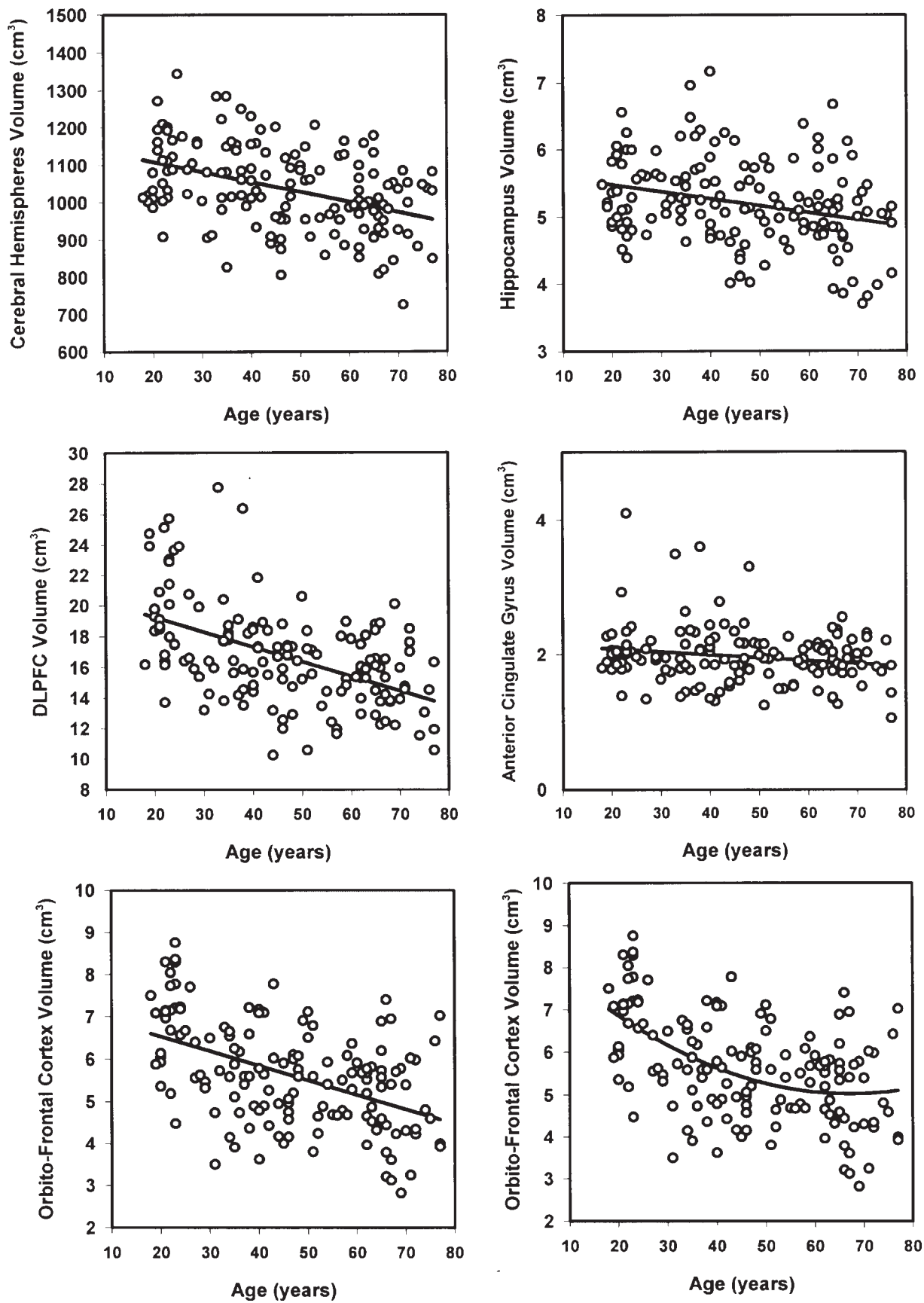
Figure 5. (A–C) Scatter plots and simple linear regressions of regional brain volumes on age. For orbito-frontal cortex both significant components – linear and quadratic – are depicted in (A) above.
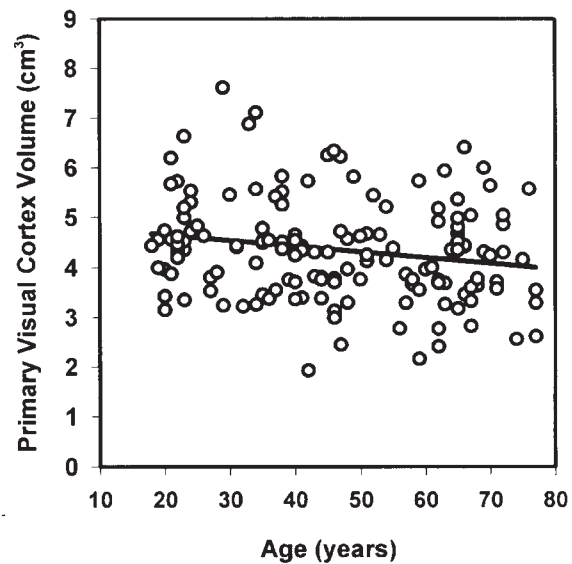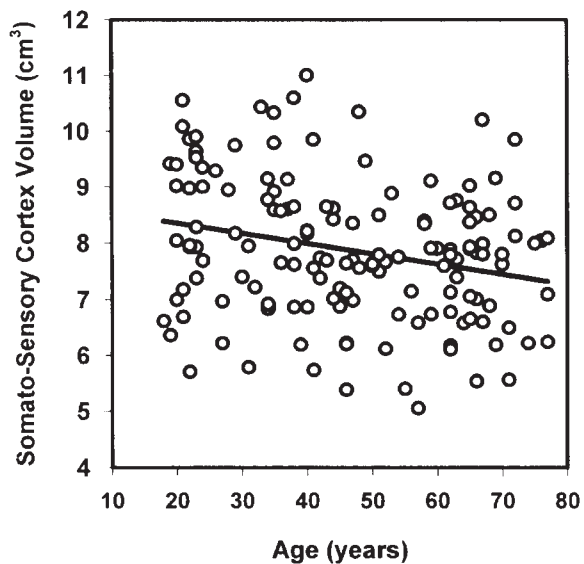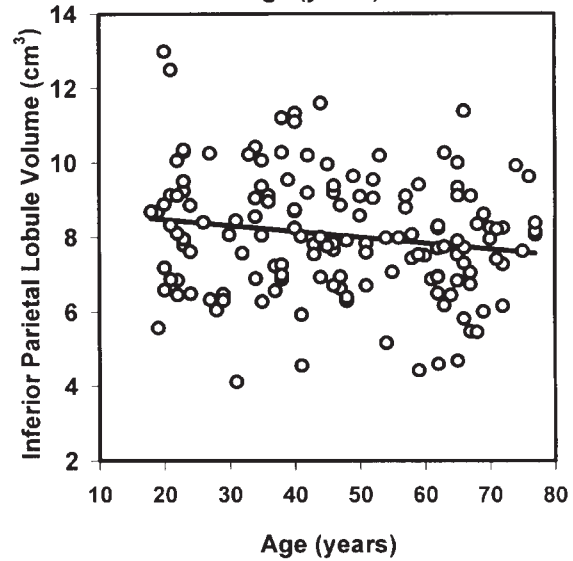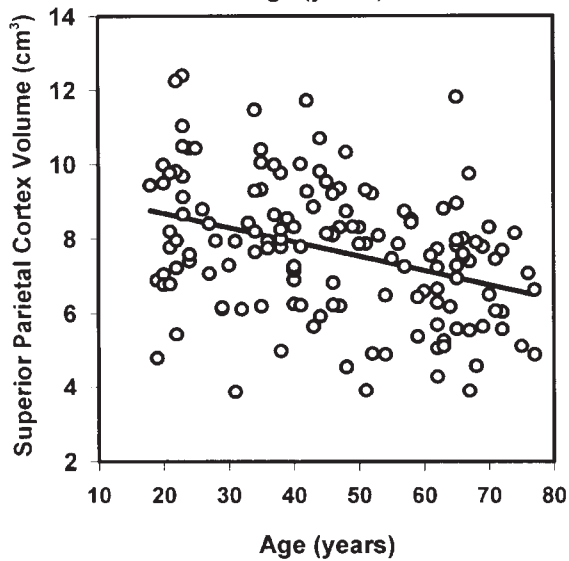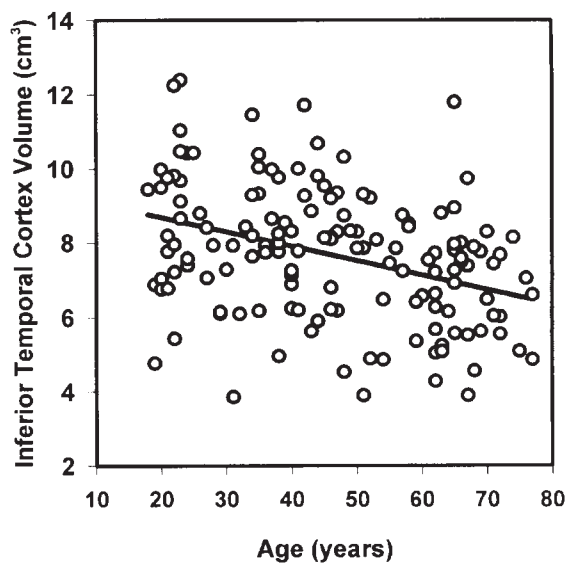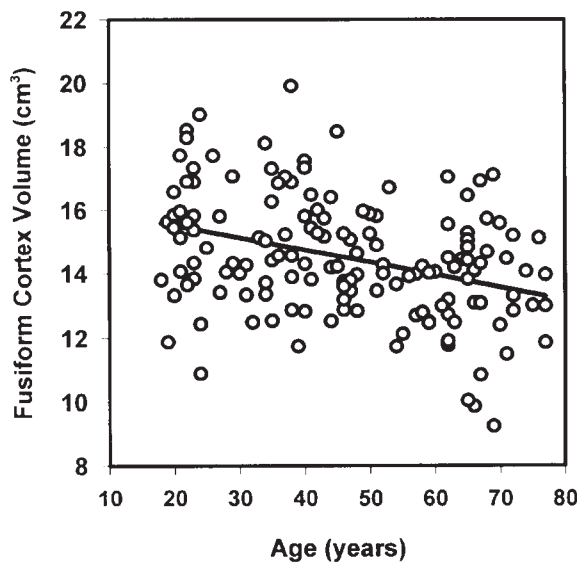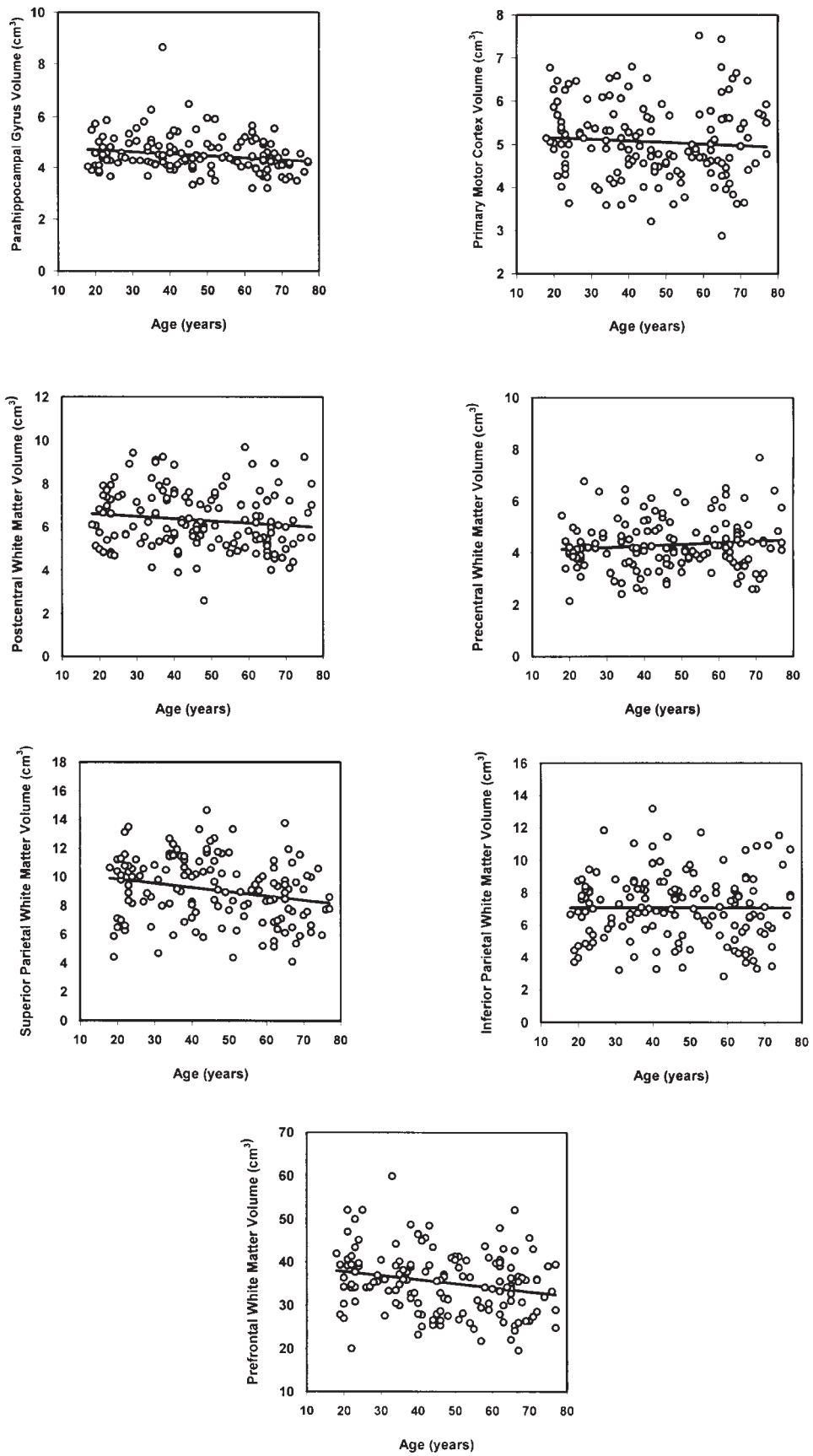
Figure 5*B*

Figure 5*C*

larger on the left, while the reverse was true for the superior parietal cortex. The parahippocampal and the pericalcarine cortices were larger in the left hemisphere, whereas the fusiform gyrus was larger on the right. None of the measured ROIs exhibited clear hemispheric differences in age-related shrinkage. The strongest evidence of (right) hemi-aging was observed for the superior parietal white matter. The semipartial correlations between the latter region's volume and age (controlling for height) were –0.27 for the right and –0.13 for the left, with a marginally significant hemisphere × age interaction: $F(1,144) = 5.41$, $P < 0.025$.

For frontal and occipital asymmetry (petalias) we observed the expected torque pattern: excess tissue volume in the right rostral (24.2 ± 38.2%) and left caudal (47.6 ± 75.1%) tips of the brain. The Spearman correlation between the measures of frontal and occipital petalias was $\rho = -0.43$, $P < 0.001$, indicating that people with greater asymmetry on one end of the brain were likely to exhibit a more prominent reversed asymmetry on the other end. Neither age (both $rs < 0.05$, NS), nor sex (both $ts < 1.14$, NS) had a significant effect on petalias.

When head size was substituted for height in the linear models, the pattern of the results remain essentially unchanged, with the prefrontal gray matter still showing greater age-related differences than any other ROI. However, due to greater share of common variance between the brain and the head size, the magnitude of all age effects and most of the sex effects was reduced. Specifically, the age effects on hippocampal formation, primary somatosensory cortex, prefrontal and superior parietal white matter were no longer significant. The other notable changes were appearance of significant leftward asymmetry of the hippocampal formation [only for men, $F(1,63) = 11.64$, $P < 0.001$], a significant sex difference in the anterior cingulate gyrus volume [$F(1,144) = 11.56$, $P < 0.001$], and a significant sex difference in the postcentral gyrus [$F(1,144) = 11.20$, $P < 0.001$]. Men had larger volumes in all three instances.

Discussion

Cortical Aging
The results of this prospective cross-sectional investigation support the hypothesis of differential brain aging. The observed *in vivo* pattern of regional stability and decline in the cerebral cortex replicates and extends our previous findings (Raz *et al.*, 1993a) as well as the PM literature. The PFC exhibits greater sensitivity to aging than the rest of the cerebral cortex. Other polymodal and visual association cortices (superior parietal, inferior temporal and fusiform) evidence sizeable but significantly milder age-related declines, whereas primary sensory and motor areas are either minimally affected or remain intact throughout life. The exceptions to this rule are the parahippocampal gyrus and the inferior parietal lobule, both polymodal association areas that, in this sample, showed little change with age. The results of rCBF studies (Grady *et al.*, 1994, 1995) suggest that the dorsal (occipito-parietal) visual pathway may be more sensitive to the effects of age than its ventral counterpart, which includes the inferior temporal and the fusiform gyri. They also suggest that aging may be associated with weakening of connections between the two areas. Our findings provide only partial support for this hypothesis as both superior parietal and inferior temporal-fusiform regions are equally and moderately affected by aging.

Somewhat surprising is the lack of more substantial age-related differences in the limbic regions — the hippocampal formation and the anterior cingulate gyrus. Animal and human PM studies reveal age-related changes in the hippocampus (Landfield, 1988; Kemper, 1994), and although some exceptions have been reported (Sullivan *et al.*, 1995), it is unlikely that in healthy humans this structure is age insensitive. The hippocampus is a complex structure, and its distinct subdivisions evidence differential aging rates. The magnitude of the correlations between age and neuronal count in specific areas of the hippocampus vary as widely as the age trends among the cortical ROIs in our sample: the $r = -0.46$ for subiculum is balanced with $r = -0.11$ for the CA1 field, with the median correlation of $r = -0.21$ (West, 1993). A small age-related decline in the total hippocampal volume ($r = -0.28$) observed in our sample is comparable to the age effects on the hippocampus reported in West's study. Thus, our findings for the hippocampal formation are in line with what is reported in the literature, and the perception of discrepancy arises from the fact that PFC shows even greater age-related declines.

The biological mechanisms underlying the observed differential aging of the cerebral cortex are unknown. All major monoaminergic neurotransmitter systems of the brain can be implicated to some degree in promoting selective cortical aging by mediating the loss of neurons in cortical targets through age-related atrophy of their subcortical sources (Bartus *et al.*, 1985; Kemper, 1993; McGeer *et al.*, 1990; Manaye *et al.*, 1995). Although substantial neurochemical and neuropharmacological evidence implicates monoamines, and especially dopamine, in selective brain aging (Goldman-Rakic and Brown, 1981; De Keyser *et al.*, 1990; Kalaria *et al.* 1989; Kalaria and Andorn, 1991; Wong *et al.*, 1984; Scarpace and Abrass, 1988; Amenta *et al.*, 1990, 1994), other findings suggest a more generalized pattern of age-related changes in cortical neurochemistry (Blin *et al.*, 1993; Bigham and Lidow, 1995; Williams and Goldman-Rakic, 1993). A model of brain aging based on central cholinergic dysfunction (Bartus *et al.*, 1985) is even less likely to account for the observed pattern of differential cortical aging, for it predicts age-related deterioration of structures that receive dense cholinergic projections from the nucleus basalis of Meynert — the hippocampus, prefrontal cortex, parahippocampal and cingulate gyri, and the insula (Mesulam *et al.*, 1984; Wenk *et al.* 1989).

The pattern of selective cortical aging reported here resembles the map of brain distribution of growth-associated protein (GAP-43), which is considered a marker for neural plasticity. The highest concentrations of GAP-43 have been observed in the association cortices, and only a minimal amount was detected in the primary sensory areas (Neve *et al.*, 1988), and GAP-43 expression is reduced with age (Ostereicher *et al.*, 1988). If neural plasticity is driven by changes in Ca^{2+} flow (Lynch and Baudry, 1991), neurons characterized by a greater ability to change Ca^{2+} current may be better suited for structural changes. However, the influx of the same ion is also responsible for excitotoxicity and, eventually, in cell death (Landfield, 1988; Dubinsky, 1993). Therefore, areas of greater plasticity may be especially vulnerable to aging. The primary neuronal membrane glycosphingolipids — gangliosides — play an important role in synaptogenesis and repair of the neurons, and the pattern of their age-related decline resembles the map of cortical aging observed in this sample (Kracun *et al.*, 1992). This observation suggests that selected cortical regions, such as the PFC, may suffer accelerated aging because of an impaired ability of the neurons that populate them to repair the damage and to alter their connectivity patterns.

Selectivity of brain aging may have evolutionary and ontogenetic underpinnings. Age-sensitive regions of the neocortex are the latest phylogenetic additions to the brain, whereas the primary sensory areas have changed little in the course of mammalian evolution (Armstrong, 1990; Sarnat and Netsky, 1981). In early development, age-sensitive cortical regions also tend to mature later than the areas relatively spared by aging (Huttenlocher, 1990; Koop *et al.*, 1986; Semenova *et al.*, 1989). Thus, increased vulnerability to aging may be the price for increased developmental malleability of some cortical areas.

Methodological Limitations

In interpreting the results of this and other *in vivo* MRI studies, we must take into account several methodological limitations.

First, the neurohistological meaning of age-related differences in the gross volume of cerebral tissue observed on the MRI remains unclear. Without exception, in all regions that evidenced age-related differences in tissue volume, the gray matter appears more sensitive to aging than the white matter. Selective vulnerability of brain tissue to aging may serve as an example of *pathoclisis*, a concept proposed by Vogt and Vogt (1951), who argued that some gray matter structures (grisea) have increased susceptibility to pathogens. The observed reduced volume of the cortical ribbon may reflect loss of neuronal bodies, decrease in their volume or thinning of the dendritic arbor. It is unlikely to indicate the loss of glial cells, for in contrast to the evidence of age-related neuronal loss, neuronal shrinkage and dendritic atrophy (Coleman and Flood, 1987; Flood and Coleman, 1988), the glial population may increase with age (Devaney and Johnson, 1980; Peters *et al.*, 1991; Landfield *et al.*, 1977). Moreover, gliosis associated with cumulative regional neuropathology would have increased the volume of the ROIs, and would not contribute to age-related shrinkage. In contrast, regressive changes in the dendritic arbor may account for senescent reduction in cortical volume, especially in the areas where the size of the cortical ribbon does not stabilize in infancy, but grows into adolescence. Such growth (as observed in the PFC) cannot reflect addition of neurons. It can be produced only by proliferation of astroglia, expansion of vasculature or increase in dendritic arborization (Purves, 1994). Therefore, with glia excluded as a contributor to age-related reduction in gross cortical volume, vascular changes and, especially, recession of the dendritic arbor appear to be good candidates to explain age-related neuroanatomical regression.

Throughout the brain we observed modest, if any, age-related declines in the regional white matter volume. Although these findings are consistent with almost all published MRI studies, their interpretation is not simple. The gross white matter volumes measured in these studies are determined by multiple factors with opposing influence. Aging is associated with the loss of myelin (Ansari and Loch, 1975) – a process that is expected to bring reduction of the white matter volume. On the other hand, a parallel process of expansion of the capillary network and swelling of perivascular spaces (Meier-Ruge *et al.*, 1992) is likely to cause increases in the volume of tissue identified on T_1-weighted MRI scans as white matter.

The second neuroanatomical limitation is that although our approach to delineation of cortical ROIs by gross neuroanatomical criteria and landmarks is better in accommodating individual variability than automated, template-based methods (Rademacher *et al.*, 1992, 1993), it still lacks the confidence of the methods used in animal studies (Felleman and Van Essen, 1991). Although our study is an incremental step in approaching the goal of mapping human brain in aging and development, we can only hope that its results will be confirmed with more refined methods of *in vivo* neuroanatomy that are being developed.

The third limitation stems from the design of the study. This is a cross-sectional investigation in which age differences observed at a given time are used to make inferences about the aging process. Such studies have known limitations. The main threat to the validity of our conclusions lies in possible confounding of age differences and cohort effects. Specifically, a secular trend in brain growth (Miller and Corsellis, 1977) may account for what we viewed as age-related declines. Nothing short of a longitudinal study can alleviate this concern completely. We do believe, however, that secular trends in brain growth are unlikely to influence our findings. First, the brain increase within the span of the last generations coincides with the general increase in body size. Furthermore, Haug (1987) estimated that secular increases in stature are 1 mm/year, which amounts to ~0.6%/decade. The added growth of the brain is estimated at 0.6 cm^3/year or ~0.5%/decade. Secular increases as such are smaller by an order of magnitude than age-related differences observed in this sample. In any case, by covarying height, we removed at least a substantial fraction of secular trend variance from the volume–age relationships. Second, the secular increase is unlikely to influence selected parts of the brain. Therefore, even if there were a considerable contribution of generational changes in general brain and body size, the relative pattern should still be preserved.

Sex Differences

The results of this study in general do not support the hypothesis of accelerated age-related declines in men. The volume of the whole cerebrum and at least one of its regions (the hippocampus) were larger in men, regardless of age, and in other parts of the cortex the nonsignificant trends invariably favored men, in spite of adjustment for rather large differences in body size (stature). Only in one region (IT) was the age-related decline in volume marginally steeper in men, with the hippocampus showing a trend in the opposite direction. It is important to emphasize, however, that examination of sexually dimorphic properties of the brain in this study was constrained by our sampling strategy. We concentrated on recruiting healthy participants of both sexes, and probably made the resulting sample less then optimal for examination of sex differences in aging. Because sex is associated with differential risk for age-related diseases, it is possible that the men selected for this study were more atypically healthy than women. Such selection bias could have obscured sex differences in aging trends.

The observed sex differences in brain volume replicate brain weight findings reported in PM literature (Ankney, 1992). The magnitude of sex differences in cerebral size ($d = 0.93$)[2], is not significantly different from those reported in other MRI studies of lifespan samples (Shah *et al.*, 1991; Gur *et al.*, 1991; Raz *et al.*, 1993b; Jäncke *et al.*, 1995). [We used Hedges and Olkin's (1985) index corrected for sample-size (effect size, d) to estimate the magnitude of sex differences. Hedges' d is a modification of Cohen's (1988) d and represents the difference between group means normalized by the pooled standard deviation and multiplied by the correction factor.] A study on a considerably smaller sample (Bhatia *et al.*, 1993) revealed a sex difference twice as large. The latter group of investigators also found sex differences of ~0.75 of standard deviation in the hippocampal

volume, which are comparable to the differences observed in this sample.

It is possible that true but small sex differences could have been obscured by increased variability of structure size. Specifically, in our sample, there was a negative correlation ($\rho = -0.54$, $P < 0.05$) between the rank-ordered magnitude of sex effect (F value in the linear model) and the rank-ordered coefficient of variation (CV, i.e. the ratio of the standard deviation to the mean). Thus, sex differences were more likely to be detected in the ROIs with lesser variability. Given excellent reliability of the measures, the issue becomes the validity of the representation of the real structures by their MRI images. For instance, when sampled at the same rate, smaller structures are represented less accurately than their larger counterparts, and could have been more prone to bias against the alternative hypothesis. This argument, however, does not hold for sex differences for there was no relationship between the magnitude of sex effect and the ROI size: $\rho = 0.07$, NS.

Cerebral Asymmetry

Most of the cerebral asymmetry findings in this sample of consistent right-handers are in accord with expectations based on the recent findings in functional neuroimaging and the lesion literature. However, our finding of leftward asymmetry in the parahippocampal gyrus is contrary to the previously reported rightward bias (Weis *et al.*, 1989). The rightward asymmetry of the whole brain replicates the PM (von Bonin, 1962) and MRI (Weis *et al.*, 1989; Gur *et al.*, 1991; Giedd *et al.*, 1996) findings, and is inconsistent with our previous report of a left-hemisphere bias (Raz *et al.* 1993b). The reason for this discrepancy is unclear, although it is plausible that lack of off-line correction for head rotation and limited sampling of the brain volume in our 1993 study could account for the asymmetry reversal. The very modest magnitude of asymmetry (~1%) makes it sensitive to even small differences in methodology.

The cerebral ROIs measured in this sample have been implicated in a variety of functions, some of them strongly lateralized (Petersen *et al.*, 1988; Price *et al.*, 1994; Petrides *et al.*, 1995; Corbetta *et al.*, 1993; Roland and Gulyás, 1995; Fiez *et al.*, 1995; Smith *et al.*, 1995). It is possible that areas that are crucial for these specialized cognitive skills have developed consistent, albeit small, hypertrophy both in evolution of the species and in development of the individuals. This thesis, however, cannot explain relative volumetric stability of the IPL, which plays a critical role in speech comprehension, working memory and verbal fluency (Gourovitch *et al.*, 1995; Smith *et al.*, 1995). Studies in which volumetric and functional asymmetries are correlated in normal subjects who undergo functional MRI and PET studies are necessary to clarify the relationship between structural and functional asymmetries.

In summary, the results of this study provide evidence of regional differences in aging of the human cerebral cortex. Determining the biological mechanisms from which this pattern emerges, and elucidating its relevance to cognitive aging is the challenge for future research.

Notes

Address correspondence to Naftali Raz, Department of Psychology, The University of Memphis, Memphis, TN 38152, USA.

References

Amenta F, Caviled C, De Michele M, Ricci A, Vega JA (1990) Changes in dopamine sensitive cyclic AMP-generating system in the rat hippocampus as a function of age. Arch Gerontol Geriat. 10:279–285.

Amenta F, Bongrani, Cadel, Ricci A, Valsecchi, Zeng (1994) Pharmacology of aging processes: Methods of assessment and potential interventions. Ann NY Acad Sci. 717:33–44.

Ankney CD (1992) Sex differences in relative brain size: the mismeasure of woman, too? Intelligence 16:329–336.

Ansari KA, Loch J (1975) Decreased myelin basic protein content of the aged human brain. Neurology 25:1045–1050.

Armstrong E (1990) Evolution of the brain. In: The human nervous system (Paxinos G, Editor), pp. 1–16, San Diego, CA: Academic Press.

Arriagada PV, Marzloff K, Hyman BT (1992) Distribution of Alzheimer-type pathological changes in nondemented elderly individuals matches the pattern in Alzheimer's disease. Neurology 42:1681–1688.

Bartus R, Dean RL, Pontecorvo MJ, Flicker C (1985) The cholinergic hypothesis: a historical overview, current perspective, and future directions. Ann NY Acad Sci, 444:332–358.

Best CT (1988) The emergence of cerebral asymmetries in early human development: A literature review and a neuroembryological model. In: Brain lateralization in children (Molfese D, Segalowitz S, eds), pp. 5–34. New York: Guilford.

Bhatia S, Bookheimer SY, Gaillard WD, Theodore WH (1993) Measurement of whole temporal lobe and hippocampus for MR volumetry: normative data. Neurology 43:2006–2010.

Bigham MH, Lidow MS (1995) Adrenergic and serotonergic receptors in aged monkey neocortex. Neurobiol Aging 16:91–104.

Blatter DD, Bigler ED, Gale SD, Johnson SC, Anderson CV, Burnett BM, Parker N, Kurth S, Horn SD (1995) Quantitative volumetric analysis of brain MR: Normative database spanning 5 decades of life. Am J Neuroradiol 16:241–251.

Blessed G, Tomlinson BE, Roth M (1968) The association between quantitative measures of dementia and senile change in the cerebral grey matter of elderly subjects. Br J Psychiat 114:797–811.

Blin J, Baron JC, Dubois B, Crouzel C, Fiorelli M, Attar-Lévy D, Pillon B, Fournier D, Vidailhet M, Agid Y (1993) Loss of brain 5-HT$_2$ receptors in Alzheimer's disease: *in vivo* assessment with positron emission tomography and [^{18}F]setoperon. Brain 116:497–510.

Bonin G von (1962) Anatomical asymmetries of the cerebral hemispheres. In: Interhemispheric relations and cerebral dominance (Mountcastle VB, ed), pp. 1–6. Baltimore, MD: Johns Hopkins Press.

Breteler MMB, van Swieten JC, Bots ML, Grobbee DE, Claus JJ, van den Hout JHW, van Harskamp F, Tanghe HLJ, de Jong PTVM, van Gijn J, Hofman A (1994) Cerebral white matter lesions, vascular risk factors, and cognitive functions in a population-based study: the Rotterdam study. Neurology 44:1246–1252.

Brody H (1955) Organization of the cerebral cortex III. A study of aging in the human cerebral cortex. J Comp Neurol 49:1–136.

Coffey CE, Wilkinson WE, Parashos IA, Soady SAR, Sullivan RJ, Patterson LJ, Figiel GS, Webb MC, Spritzer CE, Djang WT (1992) Quantitative cerebral anatomy of the aging human brain: a cross-sectional study using magnetic resonance imaging. Neurology 42:527–536.

Cohen, J (1988) Statistical power analysis. Hillsdale, NJ: Lawrence Erlbaum.

Coleman PD, Flood DG (1987) Neuron numbers and dendritic extent in normal aging and Alzheimer's disease. Neurobiol Aging 8:521–545.

Condon B, Grant R, Hadley D, Lawrence A (1988) Brain and intracranial cavity volumes: in vivo determination by MRI. Acta Neurol Scand 78:387–393.

Corbetta M, Miezin FM, Shulman GL, Petersen SE (1993) A PET study of visuospatial attention. J Neurosci 13:1202–1226.

Cowell P, Turetsky BI, Gur RC, Grossman RI, Shtasel DL, Gur RE (1994) Sex differences in aging of the human frontal and temporal lobes. J Neurosci 14:4748–4755.

DeCarli C, Murphy DGM, Gillette JA, Haxby JV, Teichberg D, Schapiro MB, Horwitz B (1994) Lack of age-related differences in temporal lobe volume of very healthy adults. Am J Neuroradiol 15:689–696.

DeCarli C, Murphy DGM, Tranh M, Grady CL, Haxby, JV, Gillette JA, Salerno JA, Gonzales-Aviles A, Horwitz B, Rapoport SI, Schapiro MB. (1995) The effect of white matter hyperintensity volume on brain

structure, cognitive performance, and cerebral metabolism of glucose in 51 healthy adults. Neurology 45:2077–2084.

DeArmond SJ, Fusco MM, Dewey MM (1976) Structure of human brain: a photographic atlas. New York: Oxford University Press.

De Keyser J, De Backer J-P, Vauquelin G, Ebinger G (1990) The effect of aging on the D_1 dopamine receptors in human frontal cortex. Brain Res 528:308–310.

Devaney KO, Johnson HA (1980) Neuronal loss in the aging visual cortex of man. J Gerontol 35:836–841.

Dubinsky JM (1993) Examination of the role of calcium in neuronal death. In: Markers of neuronal injury and degeneration (Johanessen JN, ed). Ann N Y Acad Sci 679:32–42.

Duvernoy HM (1988) The human hippocampus. An atlas of applied anatomy. Munich: Bergmann.

Felleman DJ, Van Essen DC (1991) Distributed hierarchical processing in the primate cerebral cortex. Cereb Cortex 1:1–47.

Fiez JA, Raichle ME, Miezin FM, Petersen SE (1995) PET studies of auditory and phonological processing: effects of stimulus characteristics and task demands. J Cog Neurosci 7:357–375.

Flood DG, Guarnaccia M, Coleman PD (1987) Dendritic extent in human CA_{2-3} hippocampal pyramidal neurons in normal aging and senile dementia. Brain Res 409:88–96.

Flood DG, Coleman PD (1988) Neuron numbers and size in aging brain: comparison of human, monkey, and rodent data. Neurobiol Aging 9:453–463.

Freedman M, Knoefel J, Naeser M, Levine H (1984) Computerized axial tomography in aging. In: Clinical neurology of aging (Albert ML, ed), pp. 139–148. New York: Oxford University Press.

Fukuda H, Kitani M (1995) Difference between treated and untreated hypertensive subjects in the extent of periventricular hyperintensities observed on brain MRI. Stroke 26:1593–1597.

Galaburda AM (1995) Anatomical basis of cerebral dominance. In: Brain asymmetry (Davidson RJ, Hugdal K, eds). Cambridge, MA: MIT Press.

Giedd JN, Snell JW, Lange N, Rajapakse JC, Casey BJ, Kozuch P, Vaituzis AC, Vauss YC, Hamburger SD, Kaysen D, Rapoport JL (1996) Quantitative magnetic resonance imaging of human brain development: ages 4–18. Cereb Cortex, 6:551–560.

Goldman-Rakic PS, Brown RM (1981) Regional changes in monoamines in cerebral cortex and subcortical structures of aging rhesus monkeys. Neuroscience 6:177–187.

Gourovitch ML, Kirkby B, Gold J, Esposito G, Van Dorn J, Ostrem J, Goldberg T, Weinberger DR, Berman K (1995) J Int Neuropsychol Soc 1:140.

Goy RW, McEwen BS (1980) Sexual differentiation of the brain. Cambridge, MA: MIT Press.

Grady CL, Maisog JM, Horwitz B, Ungerleider LG, Mentis MJ, Salerno JA, Pietrini P, Wagner E, Haxby JV (1994) Age-related changes in cortical blood flow activation during visual processing of faces and location. J Neurosci, 14:1450–1462

Grady CL, McIntosh AR, Horowitz B, Maisog J.Ma, Ungerleider LG, Mentis MJ, Pietrini P, Schapiro MB, Haxby JV (1995). Age-related reduction in human recognition memory due to impaired encoding. Science 269:218–221.

Gualtieri T, Hicks R (1985) An immunoreactive theory of selective male affliction. Behav Brain Sci 8:427–441.

Gur RC, Mozley PD, Resnick SM, Gotlieb GL, Kohn M, Zimmerman R, Herman G, Atlas S, Grossman R, Beretta D, Erwin R, Gur RE (1991) Gender differences in age effect on brain atrophy measured by magnetic resonance imaging. Proc Natl Acad Sci USA 88:2845–2849.

Haug H (1985) Are neurons of the human cerebral cortex really lost during aging? A morphometric examination. In: Senile dementia of Alzheimer type (Tarber, J, Gispen, WH, eds), pp. 150–163. Berlin: Springer-Verlag.

Haug H (1987) Brain sizes, surfaces, and neuronal sizes of the cortex cerebri: a stereological investigation of man and his variability and a comparison with some mammals (primates, whales, marsupials, insectivores, and one elephant). Am J Anat 180:126–142.

Hedges L, Olkin I (1985) Statistical methods for meta-analysis. Orlando, FL: Academic Press.

Heinsen H, Henn R, Eisenneger W, Gotz M, Bohl J, Bethke B, Lockermann U, Puschel K (1994) Quantitative investigation on human entorhinal cortex: left–right asymmetry and age-related changes. Anat Embryol 190:181–194.

Huttenlocher PR (1990) Morphometric study of human cerebral cortex development. Neuropsychologia 28:517–527.

Insausti R, Tuñon T, Sobriviela T, Insausti AM, Gonzalo LM (1995) The human entorhinal cortex: a cytoarchitectonic analysis. J Comp Neurol 355:171–198.

Jäncke L, Staiger JF, Schlaug G, Huang Y, Steinmetz H (1995) Body height, forebrain and hindbrain volume in 120 young adults. Soc Neurosci Abstr 21:439.

Jernigan TL, Press GA, Hesselink JR (1990) Methods for measuring brain morphologic features on magnetic resonance images: validation and normal aging. Arch Neurol 45:404–408.

Jernigan TL, Archibald SL, Berhow MT, Sowell ER, Foster DS, Hesselink JR (1991) Cerebral structure on MRI, part I: localization of age-related changes. Biol Psychiat 29:55–67.

Kalaria RN Andorn AC (1991) Adrenergic receptors in aging and Alzheimer's disease: decreased β_2-receptors demonstrated by [^{3}H]P-aminoclonidine binding in prefrontal cortex. Neurobiol Aging 12:131–136.

Kalaria RN, Andorn AC, Tabaton M, Whitehouse PJ, Harik SI, Unnerstall JR (1989) Adrenergic receptors in aging and Alzheimer's disease: increased β_2-receptors in prefrontal cortex and hippocampus. J Neurochem 53:1772–1781.

Kemper TL (1993) The relationship of cerebral cortical changes to nuclei in the brainstem. Neurobiol Aging 14:659–660.

Kemper TL (1994) Neuroanatomical and neuropathological changes during aging and in dementia. In: Clinical neurology of aging, 2nd edn (Albert ML, Knoepfel EJE, eds), pp. 3–67. New York: Oxford University Press.

Koop M, Rilling G, Herrmann A, Kretschmann HJ (1986) Volumetric development of the fetal telencephalon, cerebral cortex, diencephalon, and rhombencephalon including the cerebellum in man. Bibl Anat 28:53–78.

Kracun I, Rosner H, Drnovsek V, Vukelic Z, Cosovic C, Trbojevic-Cepe M, Kubat M (1992) Gangliosides in the human brain development and aging. Neurochem Int 20:421–431.

Landfield PA (1988) Hippocampal neurobiological mechanisms of age-related memory dysfunction. Neurobiol Aging 9:571–579.

Landfield PW, Rose G, Sandles L, Wohlstater TC, Lynch G (1977) Patterns of astroglial hypertrophy and neuronal degeneration in the hippocampus of aged, memory-deficient rats. J Gerontol 32:3–12.

Lapidot MB (1983) Is there hemi-aging? In: Hemisyndromes: psychobiology, neurology, psychiatry (Myslobodsky MS, ed), pp. 193–212. New York: Academic Press.

LeMay M (1977) Asymmetry of the skull and handedness. J Neurol Sci 32:243–253.

LeMay M (1985) Asymmetries of the brains and skulls of nonhuman primates. In: Cerebral lateralization in nonhuman species (Glick SD, ed), pp. 233–245. New York: Academic Press.

Lynch G, Baudry M (1991) Reevaluating the constraints on hypotheses regarding LTP expression. Hippocampus 1:9–14.

Manaye KF, McIntire DD, Mann DMA, German DC (1995) Locus coeruleus cell loss in the aging human brain: a non-random process. J Comp Neurol 358:79–87.

McGeer PL, McGeer EG, Akiyama H, Itagaki S, Harrop R, Peppard R (1990) Neuronal degeneration and memory loss in Alzheimer's disease and aging. In: The principles of design and operation of the brain (Eccles J, Creutzfeldt O, eds), pp. 410–431. Berlin: Springer-Verlag.

Meier-Ruge W, Ulrich J, Brühlmann M, Meier E (1992) Age-related white-matter atrophy in the human brain. In: Psychopharmacological process of aging: towards a multicausal interpretation. Ann NY Acad Sci 673:260–269.

Mesulam MM, Rosen AD, Mufson EJ (1984) Regional variations in cortical cholinergic innervation chemoarchitectonics of acetylcholinesterase containing fibers in the macaque brain. Brain Res 311:254–258.

Miller AKH Corsellis JAN (1977) Evidence for a secular increase in human brain weight during the past century. Ann Human Biol 4:253–257.

Montemurro DG Bruni JE (1988) The human brain in dissection, 2nd edn. New York: Oxford University Press.

Nebes, R.D. (1990). Hemispheric specialization in the aged brain. In: Brain circuits and the functions of the mind (Trevarthen C, ed). Cambridge: Cambridge University Press.

Neve RL Finch EA Bird ED Benowitz LI (1988) Growth-associated protein GAP-43 is expressed selectively in associative regions of the human brain. Proc Natl Acad Sci USA 85:3638–3642.

Nieuwenhuys R, Voogd J, van Huijzen C (1988) Central nervous system: a synopsis and atlas. Berlin: Springer-Verlag.

Oldfield RC (1971) The assessment and analysis of handedness. Neuropsychologia 9:97–113.

Ono M, Kubik S, Abernathey CD (1990) Atlas of cerebral sulci. Stuttgart: Thieme.

Ostereicher AB, DeGraan PNE, Gispen WH (1986) Neuronal membranes and brain aging. Prog Brain Res 70:239–254.

Peters A, Josephson K, Vincent SL (1991) Effects of aging on the neuroglial cells and pericytes within area 17 of the rhesus monkey cerebral cortex. Anat Rec 229:384–398.

Petersen SE, Fox PT, Posner MI, Mintun M, Raichle ME (1988) Positron emission topographic studies of the cortical anatomy of single word processing. Nature 331:585–589.

Petrides M, Alivisatos B, Evance AC (1995) Functional activation of the human ventrolateral frontal cortex during mnemonic retrieval of verbal information. Proc Natl Acad Sci USA 92:5803–5807.

Pfefferbaum A, Lim KO, Zipursky RB, Mathalon DH, Lane B, Ha CN, Rosenbloom MJ, Sullivan EV (1992) Brain gray and white matter volume loss accelerates with aging in chronic alcoholics: a quantitative MRI study. Alcohol Clin Exp Res 816:1078–1089.

Pfefferbaum A, Mathalon DH, Sullivan EV, Rawles JM, Zipursky R, Lim KO (1994) A quantitative magnetic resonance imaging study of changes in brain morphology from infancy to late adulthood. Arch Neurol 51:874–887.

Price CJ, Wise RJS, Watson JDG, Patterson K, Howard D, Frackowiak RSJ (1994) Brain activity during reading: the effects of exposure duration and task. Brain 117:1255–1269.

Purves D (1994) Neural activity and the growth of the brain. Cambridge: Cambridge University Press.

Rademacher J, Galaburda AM, Kennedy DN, Filipek PA, Caviness VS, Jr (1992) Human cerebral cortex: localization, parcellation, and morphometry with magnetic resonance imaging. J Cog Neurosci 4:352–374.

Rademacher J, Caviness VS, Jr, Steinmetz H, Galaburda AM (1993) Topographic variations of the human primary cortices: implications for neuroimaging, brain mapping, and neurobiology. Cereb Cortex 3:313–329.

Radloff LS (1977) The CES-D scale: a self-report depression scale for research in the general population. Appl Psychol Measure, 1:385–401.

Raz N (1996) Neuroanatomy of aging brain: Evidence from structural MRI. In: Neuroimaging II: Clinical applications (Bigler ED, ed). New York: Plenum Press.

Raz N, Millman D, Sarpel G (1990) Cerebral correlates of cognitive aging: gray–white-matter differentiation in the medial temporal lobes, and fluid and crystallized abilities. Psychobiology 18:475–481.

Raz N, Torres IJ, Spencer WD, Acker JD (1993a) Pathoclysis in aging human cerebral cortex: evidence from in vivo MRI morphometry. Psychobiology 21:151–160.

Raz N, Torres IJ, Spencer WD, Baertschie JC, Millman D, Sarpel G (1993b) Neuroanatomical correlates of age-sensitive and age-invariant cognitive abilities: an in vivo MRI investigation. Intelligence 17:407–422.

Raz N, Torres IJ, Briggs SD, Spencer WD, Thornton AE, Loken W, Gunning FM, McQuain JD, Driesen NR, Acker JD (1995) Selective neuroanatomical abnormalities in Down's syndrome and their cognitive correlates: evidence from MRI morphometry. Neurology 45:356–366.

Raz S, Goldstein R, Shah F, Hopkins T, Riggs WW, Magill LH, Sander CJ (1994) Sex differences in neonatal vulnerability to cerebral injury and their neurodevelopmental implication. Psychobiology 22:244–253.

Raz S, Lauterbach MD, Hopkins TL, Glogowski BK, Porter CL, Magill LH, Riggs WW, Sander CJ (1995) A female advantage in cognitive recovery from early cerebral insult. Dev Psychol, 31:958–966.

Roland P, Gulyás B (1995) Visual memory, visual imagery, and visual recognition of large field patterns by the human brain: functional anatomy by positron emission tomography. Cereb Cortex 5:79–93.

Sarnat HB, Netsky MG (1981) Evolution of the nervous system, 2nd edn. New York: Oxford University Press.

Scarpace PJ, Abrass I (1988) Alpha- and beta-adrenergic receptor function in the brain during senescence. Neurobiol Aging 9:53–58.

Semenova LK, Vasilieva VA, Tsekhmistrenko TA, Shumeiko NS (1989) Osobennosti ansamblevoy organizatsii kory bolshovo mozga tcheloveka ot rozhdeniya do 20 let [Peculiarities of ensemble organization of the human cerebral cortex from birth up to 20 years of age]. Arkh Anat Ghistol Embriol 97:15–24.

Shah SA, Doraiswami PM, Husain MM, Figiel GS, Boyko OB, McDonald WM, Ellinwood EH, Krishnan, KRR (1991) Assessment of posterior fossa structures with midsagittal MRI: the effects of age. Neurobiol Aging 12:371–374.

Shrout PE, Fleiss JL (1979) Intraclass correlations: uses in assessing raters reliability. Psychol Bull 86:420–428.

Smith EE, Jonides J, Koeppe RA, Awh E, Shumacher EH, Minoshima S (1995) Spatial versus object working memory: PET investigation. J Cog Neurosci 7:337–356.

Steiger JH (1980) Tests for comparing elements of a correlation matrix. Psychol Bull 87:245–251.

Sullivan EV, Marsh L, Mathalon DH, Lim KO, Pfefferbaum A (1995) Age-related decline in MRI volumes of temporal lobe gray matter but not hippocampus. Neurobiol Aging 16:591–606.

Talairach J, Tournoux P (1988) Co-planar stereotaxic atlas of the human brain. Stuttgart: Thieme.

Terry RD, DeTeresa R, Hansen LA (1987) Neocortical cell counts in normal human adult aging. Ann Neurol 21:530–539.

de Toledo-Morell L, Sullivan MP, Morell F, Spanovic C Spencer S (1995) Gender differences in vulnerability of the hippocampal formation during aging. Soc Neurosci Abstr 21:1708.

Unsal A, Witelson SF, Kigar DL, Steiner M (1995) Sex and handedness differences in change of size of the corpus callosum during normal aging. Soc Neurosci Abstr 21:17.

Uylings HBM, van Eden CG, Hoffman MA (1986) Morphometry of size/volume variables and comparison of their bivariate relations in the nervous system under different conditions. J Neurosci Methods 18:19–37.

Vogt C, Vogt O (1951) Importance of neuroanatomy in the field of neuropathology. Neurology 1:205–218.

Wahlund LO, Agartz I, Almqvist O, Basun H, Forssell L, Saaf J, Wetterberg L (1990) The brain in healthy aged individuals: MR imaging. Radiology 174:675–679.

Waldemar G (1995) Functional brain imaging with SPECT in normal aging and dementia: methodological, pathophysiological and diagnostic aspect. Cerebrovasc Brain Metab Rev 7:89–130.

Weis S, Haug H, Holoubek B, Örün H (1989) The cerebral dominances: quantitative morphology of the human cerebral cortex. Int J Neurosci 47:165–168.

Wenk GL, Pierce DJ, Struble RG, Price DL, Cork LC (1989) Age-related changes in multiple neurotransmitter systems in monkey brain. Neurobiol Aging 10:11–19.

West MJ (1993) Regionally specific loss of neurons in the aging human hippocampus. Neurobiol Aging 14:287–293.

Williams SM, Goldman-Rakic PS (1993) Characterization of the dopaminergic innervation of the primate frontal cortex using a dopamine-specific antibody. Cereb Cortex 3:199–222.

Wong DF, Wagner HN, Dannals RF, Links JM, Frost JJ, Ravert HT, Wilson AA, Rosenbaum AE, Gjedde A, Douglass KH, Petronis JD, Folstein MF, Thomas, Toung JK, Burns HD, Kuhar MJ (1984) Effects of age on dopamine and serotonin receptors measured by positron emission tomography in the living brain. Science 226:1393–1396.

Zipursky RB, Lim KO, Pfefferbaum A (1990) Volumetric assessment of cerebral asymmetry from CT scans. Psychiat Res Neuroimag 35:71–89.